REPORT No. 838

CONSIDERATION OF DYNAMIC LOADS ON THE VERTICAL TAIL BY THE THEORY OF FLAT YAWING MANEUVERS

By John Boshar and Philip Davis

SUMMARY

Dynamic yawing effects on vertical-tail loads are considered by a theory of flat yawing maneuvers. A comparison is shown between computed loads and the loads measured in flight on a fighter airplane.

The dynamic effects were investigated on a large flying boat for both an abrupt rudder deflection and a sinusoidal rudder deflection. Only a moderate amount of control deflection was found to be necessary to attain the ultimate design load on the tail. In order to take into account dynamic effects in design, specifications of yawing maneuverability or control movement are needed.

INTRODUCTION

The current use of semiempirical specifications for the determination of critical loads on the vertical tail of airplanes and the acknowledged inadequacies of this procedure have led to a great deal of interest in the theoretical approach to the problem. The equations of lateral motion of an airplane are well known (see, for example, reference 1); but because of the inability to obtain accurate values of the lateral stability derivatives the amount of labor involved in effecting the computations has made impracticable the application of the complete theory to the tail-loads problem. The important dynamic aspect of vertical-tail loads thus is entirely absent from current specifications.

The purpose of the present paper is to consider dynamic yawing loads on the basis of a restricted theory. With the restriction of flat yawing maneuvers the loads on the vertical tail that arise from abrupt deflections of the rudder or from suddenly imposed moments from any source may be determined. The loads were computed for a fighter airplane for which loads measured in flight were available, and, as evidence of the utility of the restricted theory, the computed and measured loads were compared. The importance of considering dynamic effects in the design of vertical tail surfaces is shown by computations made for a large flying boat undergoing an abrupt rudder deflection and a sinusoidal rudder deflection.

METHOD AND RESULTS

In the calculations, the theory of flat yawing maneuvers was adopted. The principal assumption of this theory is that the motion of the airplane resulting from a deflection of the rudder is confined entirely to the plane of yaw. This assumption implies low effective dihedral and may be used for most conventional airplanes. The mathematical details of the theory, a list of the basic assumptions, and definitions of the symbols used herein are given in the appendix. The resulting method is as simple as the method now specified for the calculation of loads on the horizontal tail. The method accounts for changes in the effective angle of attack of the vertical tail and thereby enables the chord load distribution to be calculated for dynamic conditions.

Fighter airplane.—Figure 1 presents time histories of the rudder deflection, transverse acceleration, and incremental tail load during an abrupt rudder deflection for a low-wing single-engine fighter airplane. The measured tail-load variation was derived from pressure-distribution data and the transverse acceleration was taken from accelerometer records. The measured data are shown for a power-on condition at 6000 feet and an airspeed of 200 miles per hour.

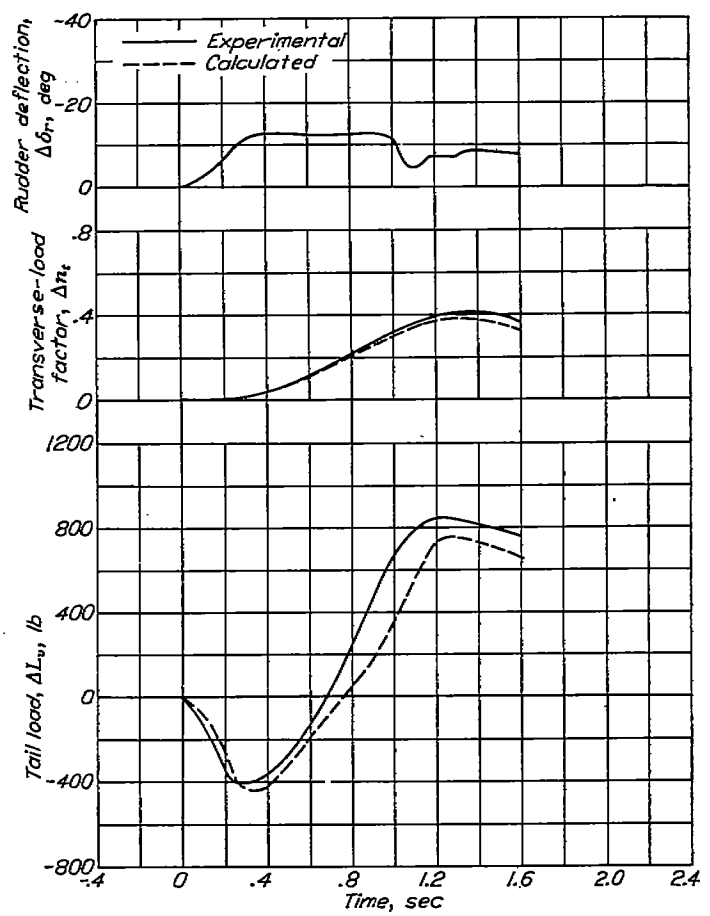

Figure 1.—Comparison of calculated and measured tail loads during rudder deflection on fighter airplane.

The measured variation of rudder angle with time was used as the forcing function in computing the theoretical transverse acceleration and incremental tail load. The aerodynamic and geometric parameters used in the computations and the source or the method by which they were obtained are given in table I. Wind-tunnel data were used wherever possible; when these data were not available, reasonable values were assigned.

Flying boat.—Calculations were made of the vertical-tail load that would be imposed on a four-engine flying boat. The loads were computed for the following two elementary types of rudder deflection: an instantaneous deflection to a constant value and a sinusoidal deflection of a frequency that would maximize the final built-up value of the load. The instantaneous rudder deflection simulates the control motion that may be used by the pilot after an engine failure. The oscillating rudder deflection corresponds to a fishtail maneuver. Both rudder deflections and the loads arising from them are shown in figures 2 and 3. The tail loads are plotted in pounds per degree of instantaneous rudder or pounds per degree amplitude of oscillating rudder. Fairly extensive wind-tunnel data were available for this airplane, and the parameters used are given in table I. The computations were carried out for a power-off condition at sea level and an airspeed of 300 feet per second.

In addition to the total maneuver load, the load and distribution on each surface of the vertical tail must be known for purposes of design. For the times indicated in figures 2 and 3, which give rise to critical loads on the rudder, fin, and total surface, chord load distributions have been computed for the flying boat by the method and charts of reference 4. The chord load distributions are presented in figure 4. The distribution in figure 4 (a) is that associated with the rudder deflected in a zero-yaw condition. Figure 4 (b) is for a condition of high angle of attack of the vertical tail and large opposite rudder deflection. Figure 4 (c) is for a high angle of attack and small rudder deflection. All types of chord

TABLE I.—GEOMETRIC AND AERODYNAMIC PARAMETERS USED IN COMPUTATIONS

Parameter	Fighter	Flying boat
Geometric		
S	236	3,686
b	37.29	200
S_v	22.9	374
W	8,100	145,000
x_v	−16.15	−65
k_z	6.05	40.6
Aerodynamic		
$dC_Y/d\beta$ $(-dC_Y/d\psi)$	[a]−0.45	[b]−0.675
$dC_n/d\beta$ $(-dC_n/d\psi)$	[a]−0.030	[b]−0.0344
$dC_L/d\alpha_v$	[c]1.43	[c]3.05
$dC_L/d\delta_v$	[c]1.10	[c]1.71
$d\sigma/d\beta$ $(-d\sigma/d\psi)$	[d]0.10	[b]−0.090
ρ	[d]0.001988	[d]0.002378
V	[d]321	[d]300
q	[d]102	[d]107
η	[d]1.00	[d]1.00
K	[d]1.00	[d]1.00

[a] Reference 2.
[b] Unpublished wind-tunnel data.
[c] Reference 3.
[d] Assigned.

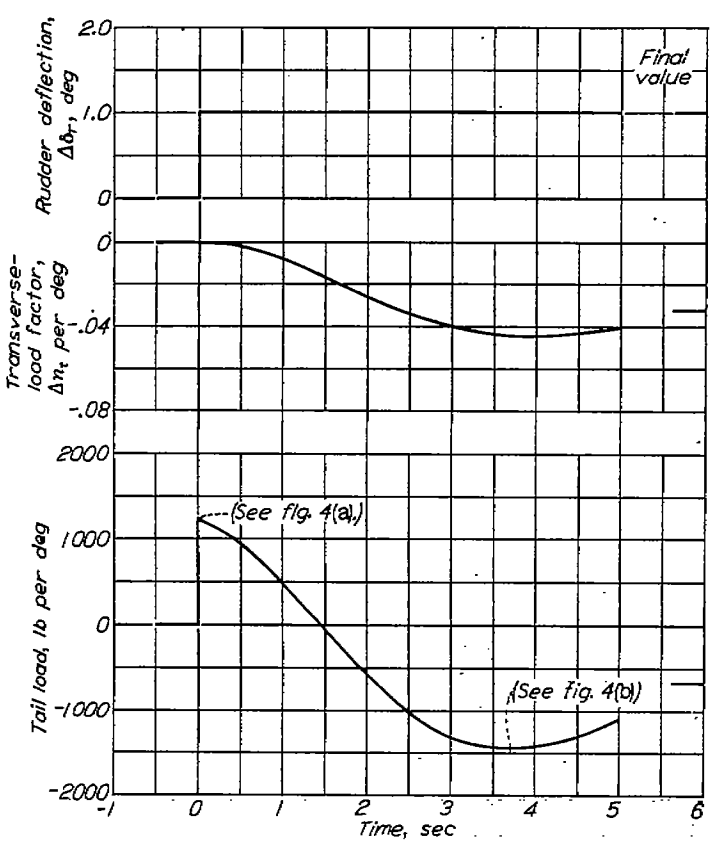

FIGURE 2.—Calculated tail load and transverse-load factor after an abrupt rudder deflection on large flying boat.

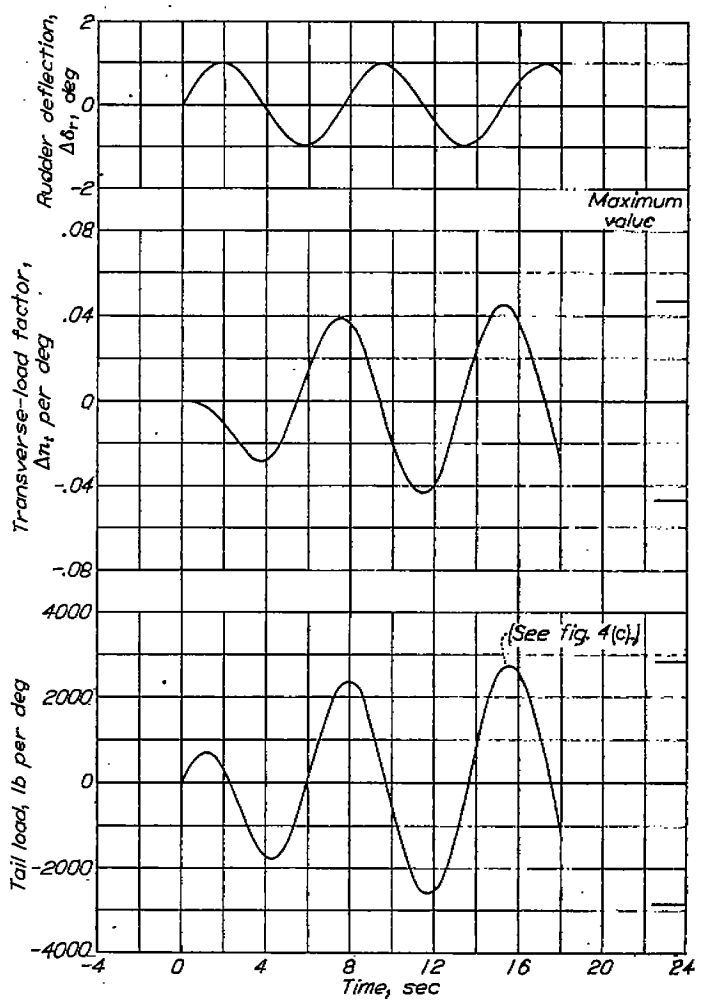

FIGURE 3.—Calculated tail load and transverse-load factor during fishtail maneuver on large flying boat.

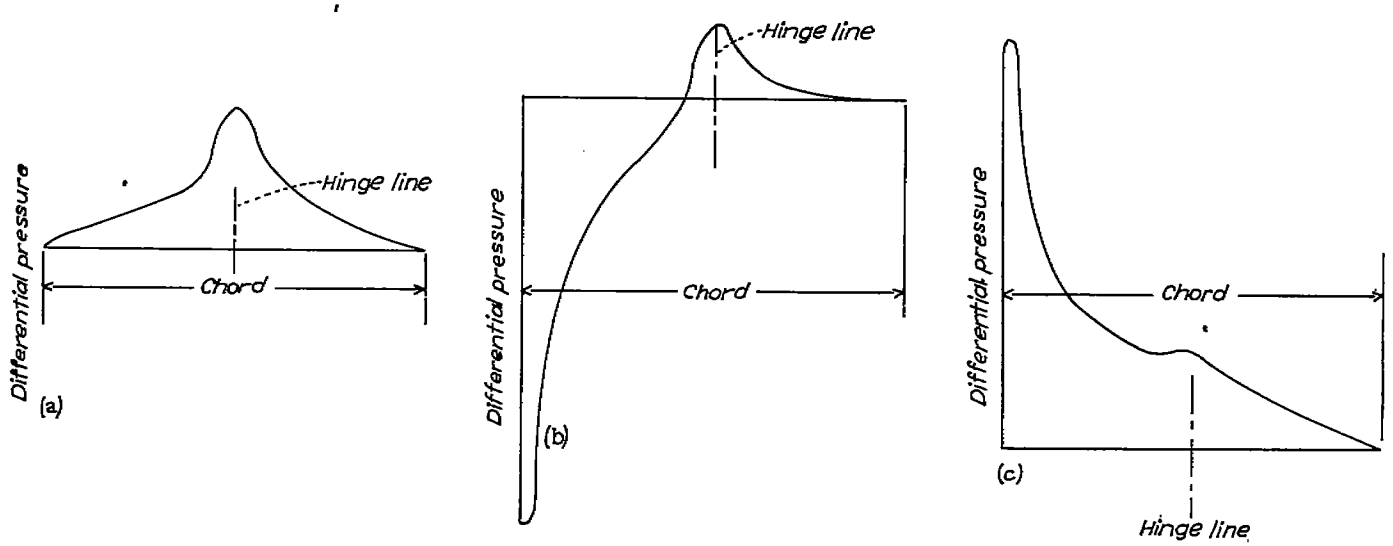

(a) Critical rudder load. Abrupt rudder deflection at zero yaw.

(b) Critical fin load. Balancing-load-type distribution; high angle of attack; large opposite rudder deflection.

(c) Critical total load. Gust-load-type distribution; high angle of attack; small rudder deflection.

FIGURE 4.—Chord load distribution over typical section of vertical tail of flying boat.

load distribution specified in present design requirements have been taken into account by these distributions; figure 4 (b) corresponds to the balancing-load condition and figure 4 (c) corresponds to the gust-load condition.

DISCUSSION

The agreement obtained between the measured and computed loads for the fighter airplane is good. Similar comparisons made for the horizontal tail of a number of widely different airplanes (reference 5), however, indicate that even with the most accurate values of parameters currently available, such close agreement of results cannot in general be expected. The availability of accurate values for the parameters involved in the equations of lateral motion seems to be on par with the availability of those used in the calculation of the loads on the horizontal tail (reference 6), and the present method is believed to provide load magnitudes that will be accurate enough for structural analysis.

The magnitude of the load resulting from an instantaneous deflection of the rudder is considerably greater than the magnitude in the final steady state, which corresponds to static conditions. This difference is shown for the flying boat inasmuch as, when dynamic effects are considered (fig. 2), an instantaneous deflection of approximately 15° is necessary in order to reach the ultimate design load obtained from current specifications; whereas when only the static conditions are considered, a rudder deflection of 33° would be necessary to reach this value. A more critical condition is that corresponding to the attainment of the ultimate design load for each surface of the vertical tail. A consideration of the critical chord load distribution (figs. 4 (a) and 4 (b)) indicates that a deflection of 13° is necessary to cause failure of the rudder although a deflection of only 10° is necessary to cause failure of the fin.

An oscillating rudder deflection of small amplitude causes large loads that are reached in a short time. The rudder motion necessary to maximize the load is very moderate because of the low natural frequency of the airplane. One cycle executed in 8 seconds is sufficient to raise the load on the vertical tail surfaces to 2400 pounds per degree (fig. 3). An amplitude of only about 9° would therefore be necessary to cause failure of the tail with this type of deflection. The initial cycle of a fishtail maneuver may be considered as a rudder reversal and its critical nature is shown by the fact that 86 percent of the load corresponding to final resonance is attained with only 1 cycle of rudder motion.

The large difference in the values of the maximum loads for the two cases considered indicates clearly the importance of the type of control-surface deflection. The importance of the type of control-surface deflection is recognized for the horizontal-tail load, and present requirements specify a standard elevator deflection to be used in combination with the airplane V–n diagram for computing critical loads (reference 7). A need is seen to exist for such a diagram for the vertical tail or for specifications of what is required of the airplane in regard to yawing maneuverability.

CONCLUSIONS

From a consideration of the dynamic yawing effects on vertical-tail loads the following conclusions are indicated:

1. When dynamic effects are considered, only a moderate amount of control deflection is necessary to reach the ultimate design load of the vertical tail surfaces of the flying boat.
2. The theory of flat yawing maneuvers provides a method for investigating dynamic loads on the vertical tail.
3. In order for theoretical developments to provide a method for the determination of critical loads on the vertical tail, they must be accompanied by specification of the yawing maneuverability that is required of the airplane.

LANGLEY MEMORIAL AERONAUTICAL LABORATORY,
NATIONAL ADVISORY COMMITTEE FOR AERONAUTICS,
LANGLEY FIELD, VA., *March 15, 1946.*

APPENDIX

DEVELOPMENT OF EQUATIONS FOR FLAT YAWING MANEUVERS

The following symbols are used:

W	airplane weight, lb
m	airplane mass, slugs
S	gross wing area, sq ft
S_v	vertical-tail area, sq ft
b	wing span, ft
k_Z	radius of gyration of airplane about yaw axis, ft
x_v	distance from center of gravity of airplane to aerodynamic center of vertical tail (negative for conventional airplanes), ft
V	true airspeed, ft/sec
ρ	density of air, slugs/cu ft
q	dynamic pressure, lb/sq ft
η	tail efficiency factor (q_t/q)
Y	force perpendicular to relative wind, lb
N	yawing moment, ft-lb; tail off
C_Y	lateral-force coefficient (Y/qS)
C_n	yawing-moment coefficient (N/qSb); tail off
β	sideslip angle (angle of plane of symmetry with relative wind), radians
ζ	flight-path angle (see fig. 5) with respect to airplane heading at start of maneuver, radians
ψ	angle of yaw, radians $(-\beta+\zeta)$
$(dC_L/d\alpha)_v$	slope of lift curve for vertical tail, per radian
$(dC_L/d\delta)_v$	rate of change of vertical-tail lift coefficient with rudder deflection, per radian
$(d\alpha/d\delta)_v$	relative rudder effectiveness
$\Delta\alpha_v$	incremental angle of attack at vertical tail, radians
δ	rudder angle measured from trim, radians
$d\sigma/d\beta$	rate of change of sidewash angle with angle of sideslip
K	empirical damping coefficient
K_1, K_2, K_3	constants occurring in basic differential equation (defined in equations (5))

The parameters $dC_n/d\beta$ and $d\sigma/d\beta$ are equal to $-dC_n/d\psi$ and $-d\sigma/d\psi$ as presented in wind-tunnel reports. The parameter $dC_Y/d\beta$ is equal to $-dC_Y/d\psi$ after $dC_Y/d\psi$ has been referred to the cross-wind axis.

In the development of the equations the following assumptions are made:

(1) The airplane is initially in steady, power-off flight.
(2) No changes in speed occur during the maneuver.
(3) No changes in altitude occur.
(4) No rolling or pitching occurs.
(5) The lateral-stability derivatives are linear functions of the angle of sideslip.

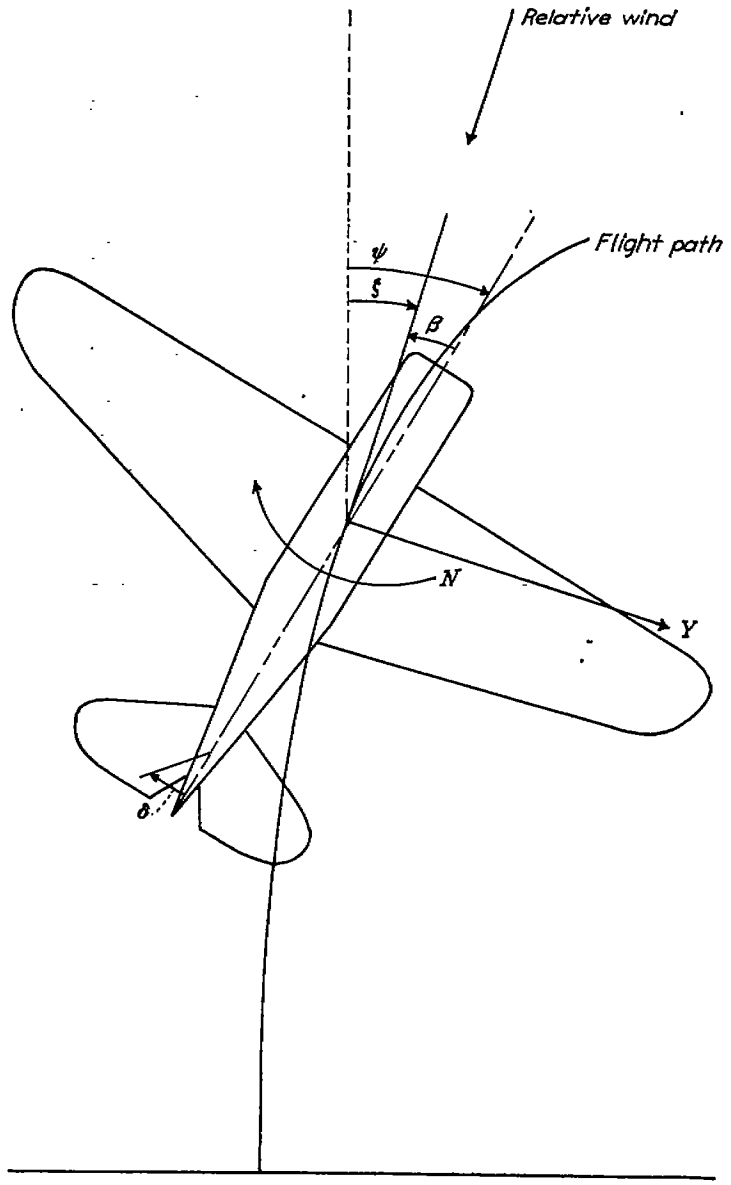

FIGURE 5.—Sign conventions employed. Positive directions are indicated by arrows.

With these assumptions the equations for the yawing motion become analogous to the equations for the pitching motion. The development of the equations parallels that given in reference 6 for the equations for an elevator deflection, and for this reason only the essential details will be indicated herein.

Equating normal forces and yawing moments to their respective accelerations results in the two conditions

$$m\dot{\zeta}V=\frac{dC_Y}{d\beta}\beta qS+\left(\frac{dC_L}{d\delta}\right)_v\eta qS_v\delta \tag{1}$$

$$\frac{dC_n}{d\beta}\beta qSb+\left(\frac{dC_L}{d\alpha}\right)_v\left[-\beta\left(1+\frac{d\sigma}{d\beta}\right)-\beta\frac{x_v}{V}\frac{d\sigma}{d\beta}-\dot{\psi}\frac{x_vK}{V\sqrt{\eta}}+\left(\frac{d\alpha}{d\delta}\right)_v\delta\right]\eta qS_vx_v=mk_Z^2\ddot{\psi} \tag{2}$$

From figure 5,

$$\psi=\zeta+(-\beta) \tag{3}$$

Combining equations (1) and (2) by use of equation (3) results in the following second-order differential equation:

$$\ddot{\beta}+K_1\dot{\beta}+K_2\beta=K_3\delta(t) \tag{4}$$

where $\delta(t)$ is the time history of the rudder deflection and

$$\left.\begin{aligned}
K_1&=\frac{\rho V}{2m}\left[\left(\frac{dC_L}{d\alpha}\right)_v\frac{S_vx_v^2}{k_Z^2}\eta\left(\frac{K}{\sqrt{\eta}}-\frac{d\sigma}{d\beta}\right)-\frac{dC_Y}{d\beta}S\right]\\
K_2&=-\frac{\rho V^2}{2m}\left\{-\frac{dC_n}{d\beta}\frac{Sb}{k_Z^2}+\left(\frac{dC_L}{d\alpha}\right)_v\eta\frac{S_vx_v}{k_Z^2}\left[\left(1+\frac{d\sigma}{d\beta}\right)+\frac{dC_Y}{d\beta}\frac{K}{\sqrt{\eta}}\frac{\rho}{2}\frac{Sx_v}{m}\right]\right\}\\
K_3&=-\frac{\rho V^2}{2m}\left[\left(\frac{dC_L}{d\delta}\right)_v\eta\frac{S_vx_v}{k_Z^2}-\left(\frac{dC_L}{d\alpha}\right)_v\left(\frac{dC_L}{d\delta}\right)_v\frac{K\eta^2}{\sqrt{\eta}}\frac{\rho}{2}\frac{x_v^2}{m}\frac{S_v^2}{k_Z^2}\right]
\end{aligned}\right\} \tag{5}$$

For an arbitrary forcing function $\delta(t)$, Duhamel's integral method described in references 6 and 7 may be used to solve equation (4). For linear forcing functions or forcing functions made up of linear segments, the method suggested in reference 8 may be employed.

The incremental vertical tail load ΔL_v is obtained from

$$\Delta L_v=\left(\frac{dC_L}{d\alpha}\right)_v\Delta\alpha_v\eta qS_v \tag{6}$$

where the effective tail angle of attack $\Delta\alpha_v$ is given by

$$\Delta\alpha_v=\left[-\beta\left(1+\frac{d\sigma}{d\beta}+\frac{dC_Y}{d\beta}\frac{\rho}{2}\frac{S}{m}\frac{x_v}{\sqrt{\eta}}\right)+\beta\left(\frac{1}{\sqrt{\eta}}-\frac{d\sigma}{d\beta}\right)+\left(\frac{d\alpha}{d\delta}\right)_v\delta\right] \tag{7}$$

and the load factor perpendicular to the flight path Δn_t is given by

$$\Delta n_t=\frac{dC_Y}{d\beta}\frac{\beta q}{W/S} \tag{8}$$

If solutions are required for a number of speeds, it may be convenient to introduce as a nondimensional independent variable $t'=\frac{t}{\tau}$, where $\tau=\frac{m}{\rho SV}$. The nondimensional spring constants K' will then be independent of the speed and will be given by

$$\left.\begin{aligned}
K_1'&=K_1\tau\\
K_2'&=K_2\tau^2\\
K_3'&=K_3\tau^2
\end{aligned}\right\} \tag{9}$$

REFERENCES

1. Weick, Fred E., and Jones, Robert T.: The Effect of Lateral Controls in Producing Motion of an Airplane as Computed from Wind-Tunnel Data. NACA Rep. No. 570, 1936.
2. Hollingworth, Thomas A.: Investigation of Effect of Sideslip on Lateral Stability Characteristics. II—Rectangular Midwing on Circular Fuselage with Variations in Vertical-Tail Area and Fuselage Length with and without Horizontal Tail Surface. NACA ARR No. L5C13, 1945.
3. Pass, H. R.: Analysis of Wind-Tunnel Data on Directional Stability and Control. NACA TN No. 775, 1940.
4. Anon.: Chordwise Air-Load Distribution. ANC-1(2), Army-Navy-Civil Committee on Aircraft Design Criteria, Oct. 28, 1942.
5. Matheny, Cloyce E.: Comparison between Calculated and Measured Loads on Wing and Horizontal Tail in Pull-Up Maneuvers. NACA ARR No. L5H11, 1945.
6. Pearson, Henry A.: Derivation of Charts for Determining the Horizontal Tail Load Variation with Any Elevator Motion. NACA Rep. No. 759, 1943.
7. Perkins, Courtland D.: Non-Dimensional Chart Method for Computing the Maneuver Loads on the Horizontal Tail Surfaces of Airplanes. AAF TR No. 4925, Matériel Command, Army Air Forces, May 13, 1943.
8. Kelley, Joseph, Jr., and Missall, John W.: Maneuvering Horizontal Tail Loads. AAF TR No. 5185, Air Technical Service Command, Army Air Forces, Jan. 25, 1945.